Experimental study on flow characteristics of compound-braided river channel

Jing Zhang[1,2] , Qin Tong[1,2], Dong Wang[3], Bo Xiang[3], Zhixue Guo[4*], Xiaoyan Gan[1,2], and Xia Wen[1,2]

[1]Key Laboratory of Fluid and Power Machinery(Xihua University), Ministry of Education.

[2]Key Laboratory of Fluid Machinery and Engineering(Xihua University), Sichuan Province.

[3]Sichuan Highway Planning, Survey, Design and Research Institute Ltd.

[4]Sichuan Univ, State Key Lab Hydraul & Mt River Engn.

Zhixue Guo (413549644@qq.com)

Key Points:

- The flow structure and flow field characteristics of Compound-Braided River model are studied.
- The secondary flow of the compound section within the influence range of bifurcated flow was obviously inhibited.
- After the bifurcated river forms the compound section, the flow resistance boundary varies, resulting in the change of the diversion ratio.

Abstract

Braided rivers easily form wide and shallow floodplains when there is no constraints on both sides of the river. During floods, rising water level submerges the floodplain of the bifurcated channel, resulting in the Compound-Braided River. The generalized model was established based on statistical data from the braided river reach of Heilongjiang. In this paper, the flow field of the straight compound-braided river was measured in flume experiments, and then the effect of the interaction of floodplain and main channel on the flow pattern, water level, flow structure and resistance force were studied under overbank flow conditions. The split ratio variation trend is further discussed. The results show that hydraulic factors in diverge segment were mainly related to braided reach, with high longitudinal velocity observed in inner floodplain. The exchange flow between floodplain and main channel accelerates transverse flow and promotes sediment transport intensity laterally. Secondary flow of compound section within the influence range of bifurcated flow was obviously inhibited. Boundary shear stress analysis showed that the diversion ratio of the main tributary under overbank condition decreased slightly and would maintain constant values as surface rise.

Keywords: Compound cross section; Braided River; Flow characteristics; Boundary shear stress; Diversion ratio

1 Introduction

The existence of center bar and floodplain will alter the channel boundary, affecting the characteristics of flow field and river process, which will bring challenges for river related work, such as navigation engineering, river regulation engineering, land use, and the development and utilization of water resources. For both of bifurcated river and compound river, numerous studies were conducted via experiments and mathematical stimulations.

For the bifurcated channel, the flow pattern at the bifurcation is the most complex and the diversion ratio affects the trend of river process. Therefore, the studies focused on the flow field characteristics of the bifurcated region, and the diversion ratio. Experimental studies of right-angle bifurcation had shown that the curvature of flow increases and the streamlines became denser when closer to the bifurcation, and the bottom and near-bottom flow patterns were different from the surface(F. Luo et al., 1995). The near-bottom flow was affected by turbulence, which complicated the flow near the bottom(ZHANG et al., 2021). In the straight braided rivers, the turbulent flow was strongest in the recirculation zone at the bifurcation, and the contour line of the high turbulence zone tended to be concave bank to convex bank from the bottom to the surface. The turbulence in the confluence segment was also strong(Hua et al., 2009; Khan & Sharma, 2019), and vortex appears at the confluence and the intensity decreases as the water flows downstream(X. Liu et al., 2019; H. Tang et al., 2018). The diversion ratio is an important hydrodynamic index in the braided river. Starting from energy, Ramamurthy studied the relationship between the diversion ratio and Froude number, and proposed a theoretical calculation formula(Ramamurthy & Satish, 1988). Tong proposed a diversion ratio estimation formula based on erosion-deposition balance and momentum conservation(TONG et al., 2011). Scholars have studied the influence of different factors on the diversion ratio through theoretical analysis and model tests, such as flow, roughness, inlet angle and branch ratio(Du et al., 2016; ZHAO et al., 2022).

For the compound section, scholars focus on the flow capacity of the section under the interaction between the floodplain and the main channel. Through experiments, Zheleznyakov found that the interaction between the floodplain and the main channel flow will reduce the

water capacity of the main channel and increase it in the floodplain(Г.B.Zheleznyakov, 1956). This was because the momentum exchange between the floodplain and the main channel changes the distribution of boundary shear stress, which affects the water transport capacity of the floodplain and main channel(HU & JI, 1999). From experimental studies of the flow structures, Proust found that small transverse flows can also affect the transverse shear layer at the junction of the floodplain and the main channel of the compound channel(Proust & Nikora, 2018, 2020). Abbaspour and Naik et al. proposed a model for predicting boundary shear stress based on experiments(Abbaspour, 2020; Naik et al., 2018). The traditional calculation method of flow capacity was no longer suitable for compound section(Stephenson & Kolovopoulos, 1990). Scholars have put forward a large number of compound river flow estimation models through model tests, theoretical analysis or numerical simulation(X. Tang, 2019; Yonesi et al., 2022).

Wide and shallow floodplains were easy to produce in bifurcated rivers when there was poor anti-scourability and no constraints on either side of the river. During the dry season, the water flows in the main channel. During the flood season, the water level rises to submerge the floodplain and the flow section develops into the compound section(Devi et al., 2017). Heilongjiang, located in the high latitude area, is the boundary river between China and Russia. Due to the political sensitivity, there is the lack of river bank regulation projects, and has bifurcation and floodplain. During the spring flood period, the flow of the main stream increased rapidly, resulting in the water level rising to submerge the floodplain, and the formation of a compound section. The compound-braided river is controlled by the braided river type in the plane shape, and the two-dimensional flow field is affected by the interaction of the floodplain and the main channel. This type of channel has both morphological characteristics and the flow characteristics are more complicated, such as branch diversion, velocity distribution and boundary shear stress. At present, there are few studies on the superposition of these two boundary conditions, but it is likely to occur during the flood season. If there is a lack of understanding of the flow characteristics of this type of river, there will be a deviation in the judgment of the trend of river process. In this study, a generalized model of compound braided channel is established. The changes of flow characteristics and resistance distribution characteristics of braided channel after overbank flow are explored through experiments, and the influence between of the floodplain and main channel interaction on braided channel diversion is analyzed.

2 Experiment overview

In the experiment, three indexes (formula (1) ~ (3)) of bending coefficient *Ka*, width ratio *K* and length-width ratio *M* were used to statistically analyze the morphology of the compound-braided river reach of the main stream of Heilongjiang River in the study area.

$$Ka = L / l \tag{1}$$

$$K = \max(B_l, B_r) \big/ \min(B_l, B_r) \tag{2}$$

$$M = L_c / B_c \tag{3}$$

Where L is the length of the reach, l is the straight line length of the reach, B_l is the total width of the left branch of reach, B_r is the total width of the right branch of reach, L_c is the length of the center bar, B_c is the width of the center bar.

There were 144 braided reaches in the study area, of which 129 were two branches, accounting for 90%. The morphological of the two-branch reaches were analyzed by using the aforementioned indicators. As shown in Table 1, the straight bifurcation with the bending coefficient *Ka* of 1.0~1.2 accounted for 73%, and the width ratio K of 1 ~ 2.5 accounted for more than 50%. The length-width ratio M was used to describe the plane shape of the center bar, and the narrow center bar ($M > 4$) was the main type and accounted for 57%.

The design of experimental model was based on the morphological characteristics of the compound-braided river reach of the Heilongjiang. The model was straight bifurcated, the center bar was narrow and long, and the width ratio of the two branches was 1: 2 (the right branch is the main branch).

Table 1. Morphological statistics of bifurcated reaches in Heilongjiang River with two branches

bending coefficient *Ka*		width ratio *K*		length-width ratio *M*	
Index ranges	percentage	Index ranges	percentage	Index ranges	percentage
1.0～1.2	73%	1～2.5	52%	2～3	16%
1.2～1.5	22%	2.5～5	34%	3～4	27%
＞1.5	5%	5～11	14%	＞4	57%

The experiment was carried out in the State Key Laboratory of Hydraulics and Mountain River Development and Protection of Sichuan University. The layout of the test model was shown in Fig.1. Before the upstream of the flume, it was arranged with inlet pipe, triangular weir, tank and grids, and the downstream was connected with sluice gate and tailwater pool. The experiment flume is 12m long, 2m wide, 0.5m high, and 1‰ gradient. The boundary was tempered glass, and the bottom was cement plaster. The model was divided into three reaches from upstream to downstream. The length of the upstream compound river reach was 3m, and the total width of the section was 1.40m. The middle reach was the compound-braided river, which included bifurcation segment, branch segment and confluence segment. The branch segment after the diversion through the center bar was a compound section. The downstream compound river reach was 3m long, with the same shape and size as the upstream section. As shown in Fig.2, both sides of the center bar were the inner floodplain of the compound section, and the side near the wall was the outer floodplain. The junction areas of the reaches were connected by the gradient section, which was to smoothly connect from the upstream to the downstream, and the boundary of the gradient section was arc boundary.

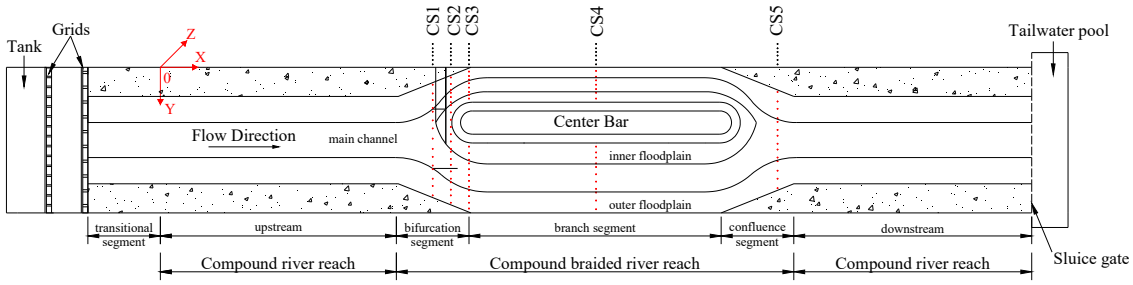

Figure 1. Plane layout of the experiment model.

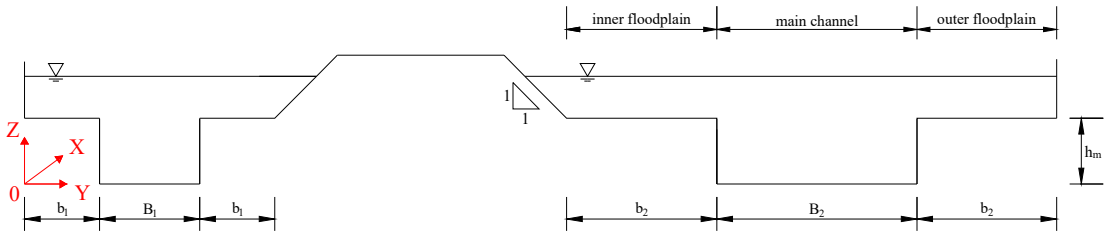

Figure 2. Cross section of the model. B is the width of the main channel, b is the width of the floodplain, and the subscripts 1 and 2 represent the left branch and the right branch respectively.

As shown in Figure 1, five typical cross-sections CS1~CS5 were set up in the study, which were located in the bifurcation segment, the branch segment and the confluence segment of the compound-braided river reach. Because the flow pattern of the bifurcation was the most complex, three cross-sections were arranged here, which were located at the beginning position of the bifurcation (CS1), the transition position of the bifurcation (CS2) and the end position of the bifurcation (CS3). The water depth was measured by using the ultrasonic water level mete, and the flow velocity was measured by using the Acoustic Doppler Velocimeter (ADV). The coordinate system setting was shown in Figure 2. The origin was located at the junction of the left side wall of the inlet cross-section and the river bottom. The X, Y, and Z axes were parallel to the river boundary, where the X axis points to the downstream, the Y axis points to the right bank, and the Z axis points to the water surface. The longitudinal velocity u points to the

downstream was positive, the transverse velocity v points to the right bank was positive, and the vertical velocity w points to the water surface was positive. The test flow range was 10~85L•s^{-1}, which was divided into 7 levels. At 10 and 15L•s^{-1}, due to the small flow rate, the floodplain was not submerged by water, which was the braided river channel. Under the other flow rates, the compound section was formed because the floodplain was submerged by water, which was the compound-braided river channel. The test conditions were shown in Table 2.

Table 2. Summary of experiment conditions

test	B_0/cm	b_0/cm	B_1/cm	b_1/cm	B_2/cm	b_2/cm	h_m/cm	Q/L·s^{-1}	river pattern
Q_1	48	36	19.2	14.4	38.4	28.8	12	10	braided river
Q_2								15	
Q_3								30	compound-braided river
Q_4								45	
Q_5								65	
Q_6								75	
Q_7								85	

Note. Where B is the width of the main channel, b is the width of the floodplain, and the subscripts 0,1 and 2 represent the unbranched river section, the left branch and the right branch respectively.

3 Results

3.1 Flow pattern of water surface

To observe the flow pattern change of the compound-braided river channel under the superposition influences between the center bar diversion and the interaction between the floodplain and the main channel. In Q_6 condition, the light colored plastic is put into the entrance of flume. Because the density of plastic is less than that of water, it can float on the water surface and move with the water flow, which can reflect the water surface flow movements of the reach. The results are shown in Figure 3.

There are ripples on the water surface in the bifurcation segment (Figure 3a) due to the jacking effect on the head of the center bar. At the junction of the bifurcation section and the branch section (Figure 3b), the water flow bypasses the head of center bar, and backflow vertical vortex appears on both sides of the center bar. The vortex of left branch is clockwise, and that of right branch is counterclockwise. The vortex moves downstream in the branch section and moves to the main channel at the same time. During the process, the vortex size continues to expand until it disappears. In the branch segment, the exposed area of water surface at the junction of the floodplain and the main channel is not covered by the plastic due to water flow mixing, as shown in Figure 3c. The exposed area of the right branch is larger than that of the left branch, indicating that the mixing of the right branch is stronger. In the confluence segment (Figure 3d), the strong mixing caused by the confluence of water flows causes the plastic to move to both sides, and an obvious mixing band appears. The exposed area in Figure 3d is the mixing band position. The mixing zone is near to the left when the water flow just confluence, and then moves to the center line of the main channel.

177 At the beginning position of the bifurcation (CS1), there is a significant water surface
178 gradient caused by the presence of the center bar. At the junction of the transition of the
179 bifurcation (CS2) and the end of the bifurcation (CS3), the water flows around the center bar and
180 produces a vertical vortex, which passes through the floodplain and main channel. The flow in
181 the branch segment is mainly affected by the interaction between the floodplain and the main
182 channel, and the flow mixing occurs at the junction of the floodplain and the main channel along
183 the reach. The flow pattern change in the confluence segment is primarily affected by the
184 confluence of water flows. Overall, the flow pattern change in the bifurcation segment is the
185 most complex due to the superposition of the center bar diversion and the interaction between the
186 floodplain and the main channel.

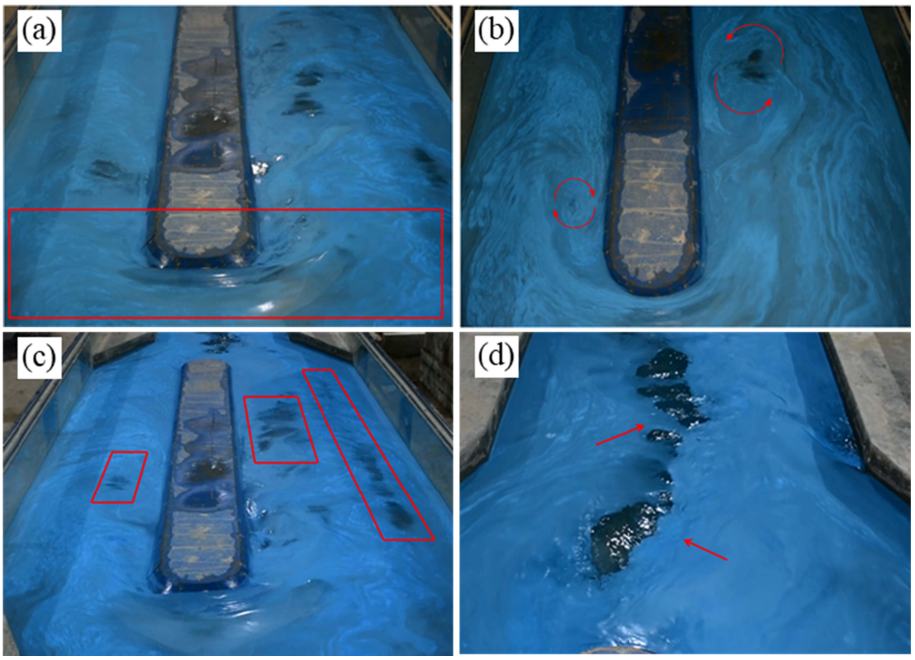

187

188 **Figure 3.** Tracing results of flow surface. (a) Jacking effect of the center bar. (b) Vortexes on
189 both sides of the center bar generate, expand and disappear. (c) Flow mixing at the interface of
190 floodplain and main channel. (d) Flow mixing band at the confluence

191 3.2 Water elevation analysis

192 When the water level rises to submerge the floodplain for the increment of discharge, the
193 width of flow section increases suddenly, varying the transverse distribution of the water level.
194 In order to compare the water level distribution along the typical sections of braided river with
195 compound-braided river, Q_2 and Q_6 group are taken as examples (see Figure 4), where the
196 floodplain is above water in Q_2 group and inundated in Q_6 group.

197 At the beginning of bifurcation (Figure 4a), the water level distribution of Q_2 group is
198 high in the middle and low on both sides because of the jacking effect of center bar, which is
199 consistent with the typical water level distribution of the braided section(H. Luo, 1989). In Q_6
200 condition, the transverse distribution of water level is also high in the middle and low on both
201 sides, but this is because the main channel of compound section has high flow velocity and water
202 level, while the floodplain has low flow velocity and low water level. Therefore, the water

surface gradient between the main channel and the floodplain on both sides is significantly greater than that of Q_2 after the influence of diversion and jacking of center bar is superimposed.

At the end of bifurcation (Figure 4b), the bending shape of the river channel has essentially terminated, which caused by the diversion, but the water flow still has strong bending characteristics because of inertia. In Q_2 group, there is high water level on the concave bank and low on the convex bank, which is consistent with the typical cross-sectional distribution of water level in curved river(Y. Liu, 2003). In Q_6 condition, the water level on the concave side is still higher than that on the convex side, and the water surface is inclined to the center bar. However, the superposition of the water surface gradient of the compound section makes the gradient between the main channel and the outer floodplain (concave bank) smaller than that between the main channel and the inner floodplain (convex bank).

The influence of channel diversion and bending completely disappears at the branch section (Figure 4c). In Q_2 condition, the water level distribution of the two branches is basically equal, which returns to the rectangular channel state. In Q_6 condition, the water level of the inner and outer floodplain is basically equal, but lower than that of the main channel, which returns to the compound channel state(Stephenson & Kolovopoulos, 1990).

In the confluence segment (Figure 4d), the flow velocity of the left branch is low due to the small discharge, so the water level on the left side is higher than that on the right when the water flow confluence. In Q_2 group, due to the small total discharge, the discharge difference between the two branches is small, so the water level of the section changes little. In Q_6 group, the discharge difference between the two branches is large, and the water level on the left side is higher than that on the right side. At the same time, the water level of the main channel is higher than that of the floodplain due to the water surface characteristics of the compound section. The mixing and collision caused by the confluence of high and low velocity water flow (see Figure 3d) and the periodic change of the vortex formed by the flow around cause the water level of the main channel to fluctuate.

Comparing the water stage of typical sections in Q_2 group with Q_6 group, it is found that the transverse distribution of the water level is mainly controlled by the compound section before and after the flow branching (Figure 4a and Figure 4c). Within the influence reach of bifurcation and confluence (Figure 4b and Figure 4d), the transverse distribution of the water level is not only controlled by braided channel, but also affected by the flow redistribution for compound section.

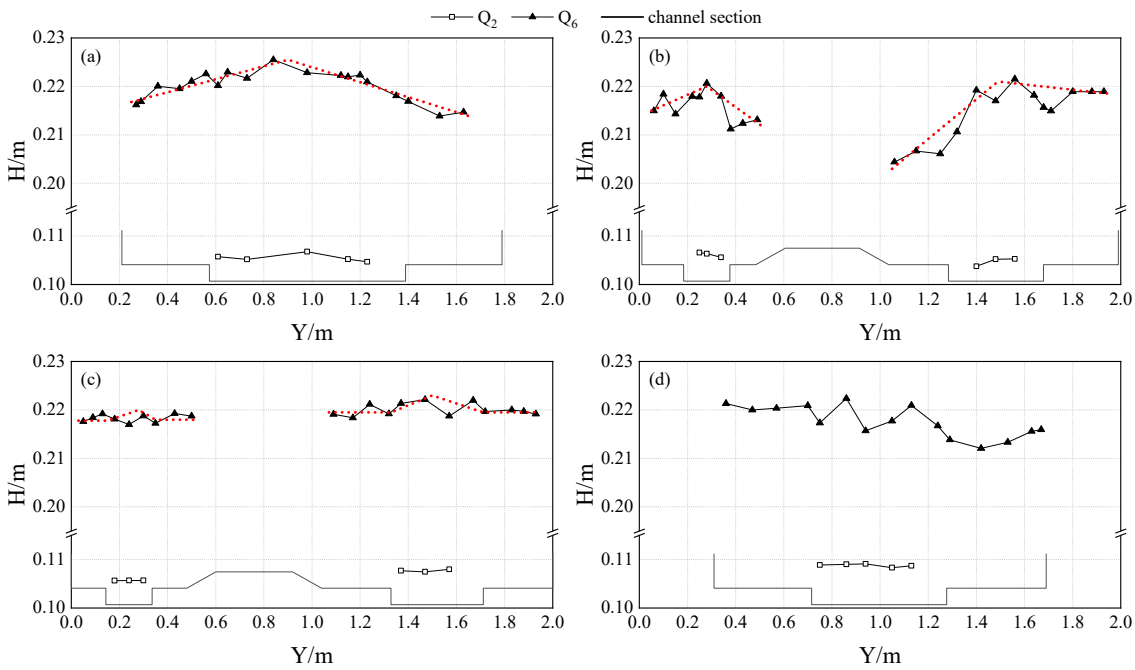

Figure 4. (a) The distribution of water level in bifurcation segment (CS1). (b) The distribution of water level in bifurcation segment(CS3). (C) The distribution of water level in branch segment(CS4). (d) The distribution of water level in confluence segment(CS5). The red dotted line is the water level trend line.

3.3 Secondary flow distribution

The vector distribution of cross-section velocity under the Q_6 condition is taken as an example. This study explores the mechanism of secondary flow generation under the superposition influence between the center bar diversion and the interaction between the floodplain and the main channel. Two vector length unit settings of 0.002 and 0.007 are used to observe the direction of the vector arrow.

The velocity vector diagram of the bifurcation section is shown in Figure 5a~Figure 5c. The streamline bending on the plane is caused by the diversion effect. The cross-section velocity vector is mainly affected by the lateral extrusion of the center bar, and the interaction between the floodplain and the main channel of the compound section is weakened, there is no circulation in the CS1. At the cross-section CS2, the water flow deflects from the head of the center bar to both sides, which makes the lateral velocity increase, and the lateral water and sediment transport is enhanced. A pair of opposite vertical vortexes is formed on both sides of the central bar head as the current separates from the flume walls (see Figure 3b). From Figure 5b, the sinking flow is formed by the flow of the inner floodplain into the bottom of the main channel, which is subjected to the centrifugal force of the vortex. The streamline plane has bending characteristics, but there is still no bend circulation. At the end of the bifurcation segment (CS3), the size of the vertical vortex increases and moves laterally to the main channel, making the water flow in the main channel more obviously downward and the angle of the sinking flow increases. At the same time, upward flow is generated in the interaction area between the main channel and the outer floodplain as the curvature of the boundary plane and the centrifugal force increase. Overall, there is no closed bend circulation at the end of the bifurcation segment. The extrusion force

caused by the diversion of the center bar makes the surface water form a transverse velocity consistent with the direction of the bottom, causing in the transverse velocity distribution of the section not conform to the law of straight or curved compound section.

When the water enters the branch segment (Figure 5d), the influence of the backflow caused by the bifurcation of the upstream center bar is very weak. The influence range of the backflow in the main branch is longer due to the larger discharge, and there are still some undercurrents on the inner floodplain into the main channel. The interaction between the floodplain and the main channel under the influence of compound section gradually increased and began to play a leading role. There is a pair of secondary flows with opposite directions at the junction of floodplain and main channel on both sides of the two branches, but its shape and position are still affected by the diversion. The circulation scale of the inner floodplain is always larger than that of the outer floodplain. The reverse circulation in the inner side of the main channel is affected by the undercurrent, which occurs above the bank water level. Moreover, the scale of secondary flow is limited by the free water surface. Only near the interaction area between the outer floodplain and the main channel, the secondary flow is nearly unaffected by the diversion.

The velocity vector diagram of the confluence segment is shown in Figure 5e (CS5). As the river width gradually narrows, water flow from both sides converges towards the central bar, resulting in an augmentation of transverse velocity. The CS5 section has been restored to the same boundary conditions as the upstream, the cross-section velocity vector is dominated by the transverse velocity generated by the confluence, and the secondary flow generated by the interaction between the floodplain and the main channel has disappeared. The cross-sectional backflow caused by the confluence of the branch flow is located on the left side of the main channel center.

In general, the velocity distribution in the branch segment located far from the diversion and confluence exhibits the typical compound cross-section characteristics. However, the strength of the secondary flow is related to the inner and outer floodplains and main channel. In the compound river reach affected by confluence, the transverse velocity is independent of the interaction between the floodplain and the main channel, and is mainly controlled by the change of the boundary plane shape. The velocity vector distribution in the bifurcation segment is also affected by center bar diversion, compound section, and plane bending, which makes more complex flow field characteristics be displayed, and the evolution of the center bar and the diversion of the branch channel are deeply affected. Therefore, the longitudinal velocity and stress distribution in the diversion segment are emphatically analyzed below.

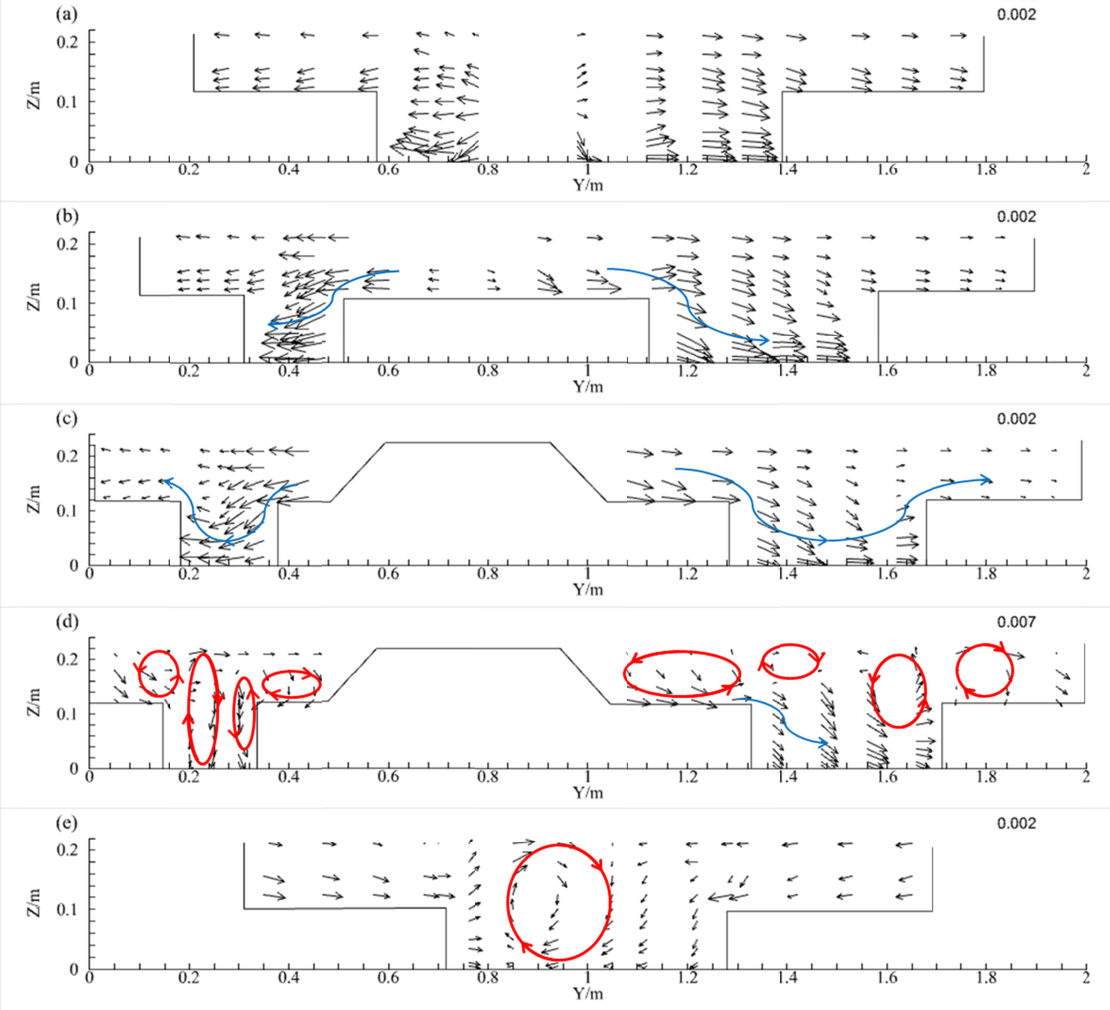

Figure 5. The velocity vector diagram of typical cross-section. (a) The velocity vector diagram of cross-section CS1. (b) The velocity vector diagram of cross-section CS2. (c) The velocity vector diagram of cross-section CS3. (d) The velocity vector diagram of cross-section CS4. (e) The velocity vector diagram of cross-section CS5. 0.002 and 0.007 are the length units of the vector arrow.

3.4 Velocity analysis in bifurcation section

The longitudinal velocity variations at three cross-sections of the beginning of the bifurcation (CS1), the transition of the bifurcation (CS2) and the end of the bifurcation (CS3) under Q6 test conditions were analyzed, as shown in Figure 6.

At the beginning of the bifurcation (Figure 6a), the velocity contour at the junction of the floodplain and the main channel is raised upward, which is basically consistent with the distribution characteristics of the longitudinal velocity contour in the compound section, but the stagnation effect of the center bar head is obvious. The high velocity area is basically at the entrance of the main branch, due to the asymmetry of the branch.

At the transition of bifurcation (Figure 6b), because the bottom in the head of the center bar is submerged, the inner floodplain of the two branches is still connected. The longitudinal

velocity distribution is consistent with the velocity distribution characteristics of the rectangular channel. The velocity distribution is basically only related to the water depth, and the overall velocity is smaller than that of the outer floodplain. The velocity gradient near the junction of the floodplain and the main channel increases suddenly. Combined with the cross-section vector of Figure 5b, the erosion of the center bar may be caused by a large transverse velocity from the junction of the floodplain and the main channel, and then the transverse transport occurs and deposits in the main channel or even the outer floodplain. In the main channel and the outer floodplain, the characteristics of the velocity contour of the compound section are basically maintained, and the contour flow core is close to the center bar due to the inertia effect of the water flow.

At the end of the bifurcation (Figure 6c), the asymmetric distribution of the flow velocity is presented at the compound section of the branch channel. The flow velocity generally decreases from the inner floodplain to the outer floodplain, which is basically consistent with the distribution characteristics of the typical velocity section after braided channel diversion, that is, the flow velocity is inversely proportional to the distance from the center bar. The flow velocity at the side wall of the outer floodplain is further lower than that of CS2, and the separation zone may appear in the downstream segment, with branch separation zone appears closer to the downstream. From Figure 5c, although there is no complete secondary flow structure, the high velocity flow of the main channel still diffuses to the outer floodplain, which results in the typical contour characteristics of the upward bulge at the junction of the outer floodplain and main channel.

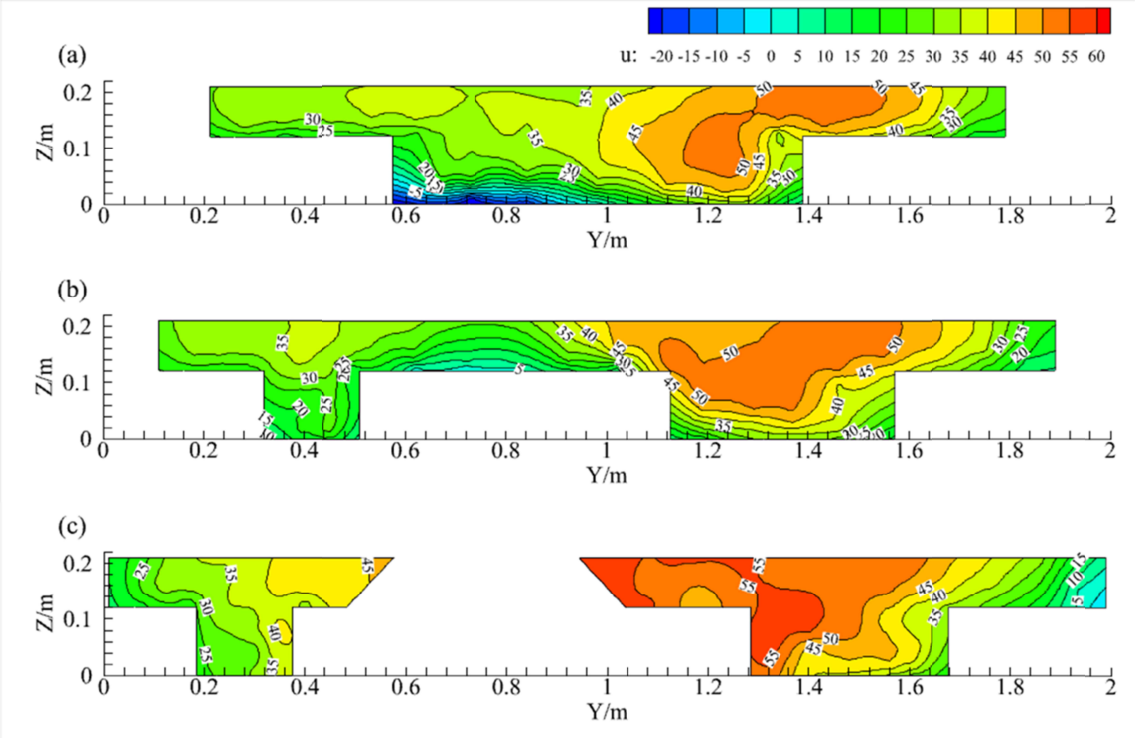

Figure 6. Longitudinal velocity variation (Q_6 condition). (a) The longitudinal velocity variation of CS1 under Q_6 condition. (b) The longitudinal velocity variation of CS2 under Q_6 condition. (c) The longitudinal velocity variation of CS3 under Q_6 condition.

During the diversion process, the longitudinal velocity distribution of the section transits from the compound section characteristics to the typical diversion characteristics. Before the complete bifurcation, the transverse velocity distribution is affected by the interaction between the floodplain and the main channel, which may affect the flow capacity of both branches. Compound-braided river channels exhibit variations in growth and decline patterns due to changes in flow capacity compared to a single rectangular section. In order to further analyze the change of the diversion characteristics under the influence of the compound section, the transverse distribution of the boundary shear stress τ_b of the CS2 section under Q_2 and Q_5~Q_7 is calculated, and the change of the resistance characteristics before and after the overbank are compared.

The boundary shear stress of compound section is generally based on the vertical average velocity U_d, which is calculated by formula (4)(LIU et al., 2012).

$$\tau_b = \rho\left(f/8\right)U_d^2 \tag{4}$$

Where ρ is the density of water and f is the Darcy-Weisbach resistance coefficient, which is calculated by Formula (5)(Spooner，Jake, 2001).

$$f = 8gn^2 \big/ R^{1/3} \tag{5}$$

Where g is the acceleration of gravity, n is the comprehensive roughness of the river section, and R is the hydraulic radius.

The determination of U_d is crucial in calculating the boundary shear stress of the compound channel. The SKM method is employed to obtain the analytical solution for the transverse distribution of U_d. In this paper, the vertical average flow velocity U_d is derived directly from the point flow velocity measurements obtained through flume tests.

The modified vertical segmentation method was utilized to calculate the hydraulic radius R, considering the impact of flow momentum exchange between the floodplain and main channel(KANG, 2023). The cross-section composition characteristics of the left and right branches are consistent, so the right branch is used as an example to illustrate the calculation parameters of the hydraulic radius R. As shown in Figure 7, the section is divided into three parts: I, II, and III. From Figure 5b and Figure 6b, it can be observed that due to blockage at the center bar head, water flow diverts towards both left and right branches at y=0.7~0.8m, and the longitudinal velocity of the two branches is basically symmetrical to the center line of the main channel. Therefore, the water body boundary on the left side of region I is replaced by the solid side wall in this paper, and the calculation parameters of I and II are completely consistent. In order to reflect the resistance effect of the floodplain flow on the main channel, the concept of equivalent wetted perimeter is used in III to appropriately increase the wetted perimeter of the boundary section between the floodplain and the main channel.

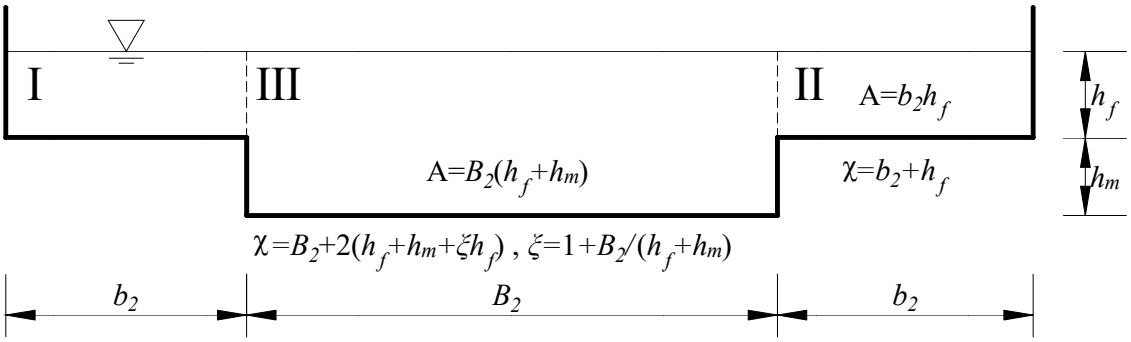

Figure 7. The diagram of section segmentation. Where A is the area calculation formula and χ is the wet cycle calculation formula.

The additional roughness in flow resistance is caused by the momentum exchange between the floodplain and the main channel. Based on the comprehensive roughness n_{LM} proposed by Lotter, KangLu further considers factors such as cross-section morphological and water depth variation, and a modified model for the composite channel comprehensive roughness is obtained by utilizing experimental data, as shown in formula (6) (KANG, 2023).

$$\frac{n}{n_{LM}} = 6\times10^{-4}\left(\frac{h_f}{h_m}\right)^{3.15}\left(\frac{B}{h_m+h_f}\right)^{2.77}\left(\frac{R}{h}\right)^{-4.59}+0.7 \tag{6}$$

The calculated values of n and R are substituted into the formula (5) to get f, and then f and U_d are substituted into the formula (4) to get the transverse distribution of the boundary shear stress τ_b of the transition of the bifurcation (CS2) of Q_2, Q_5~Q_7. The average shear stress distribution curve under three overbank flow conditions is depicted, as shown in Figure 8.

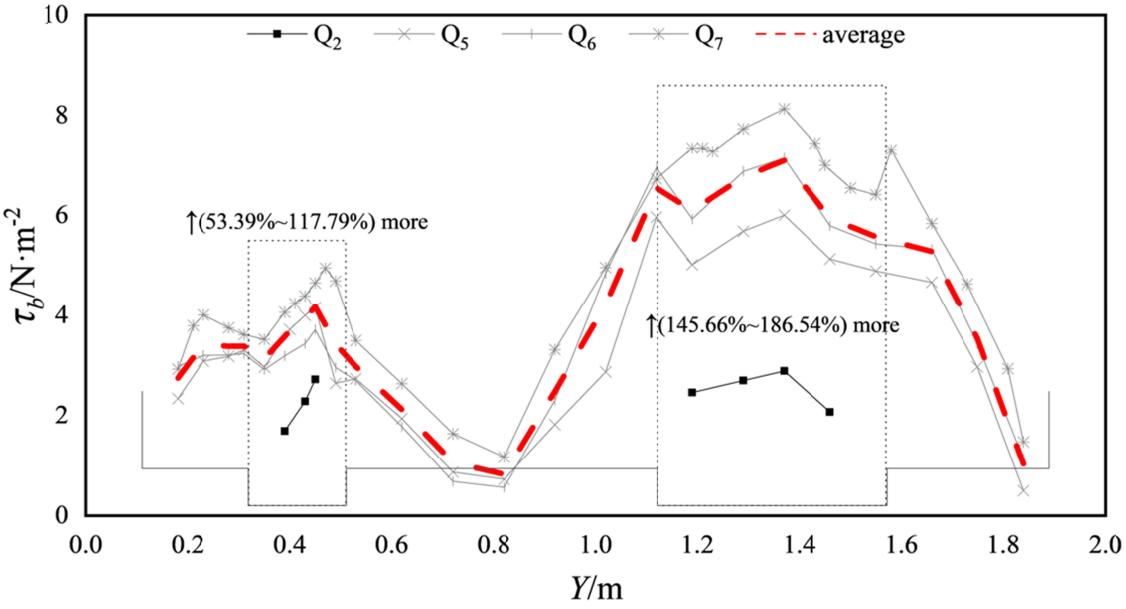

Figure 8. The transverse distribution of τ_b. The solid line is the transverse distribution of shear force under different flow conditions, in which the floodplain is not submerged in Q_2, and the floodplain is submerged in Q_5, Q_6 and Q_7 to form a compound section. The red dashed line is the

average value of the shear force for Q_5, Q_6, and Q_7. The rectangular dashed box shows the increase of the average shear force value relative to Q_2 group.

The resistance distribution of the cross section before and after the overbank is compared, as shown in Figure 8. In the main channel, the distribution trend of the shear stress remains unchanged after submergence of the floodplain. However, the resistance increases with rising water levels, particularly noticeable in the main branch where it increase at a higher rate than the other branch. The boundary shear stress of the main branch of Q_5~Q_7 increases by 145.7%~186.5% on average compared with that before the overbank, while the increase of the other branch is only 53.4%~117.8%. Furthermore, the resistance area increases due to the inundated floodplain. The ratio $(\tau_{b2}/\tau_{b1})_{inner}$ of the boundary shear stress of the inner floodplain in the main branch is about 1.71, and the ratio $(\tau_{b2}/\tau_{b1})_{outer}$ of the boundary shear stress of the outer floodplain is about 1.01. The subscripts 1 and 2 represent the branch and the main branch respectively. The main branch section is wider and the resistance area is larger, so the overbank of the rising water level will inevitably cause the resistance increase at the entrance of the main branch to exceed the branch, which may lead to the decrease of the flow proportion of the main branch.

3.5 Diversion ratio

To further compare the flow capacity of the two branches before and after the submergence of the floodplain, the main branch flow ratio $\eta=Q_r/(Q_r+Q_l)\times100\%$ is used to analyze the change of the branch diversion ratio as discharge increase, where Q_r is the main branch flow and Q_l is the other branch flow. The calculation results are shown in Figure 9.

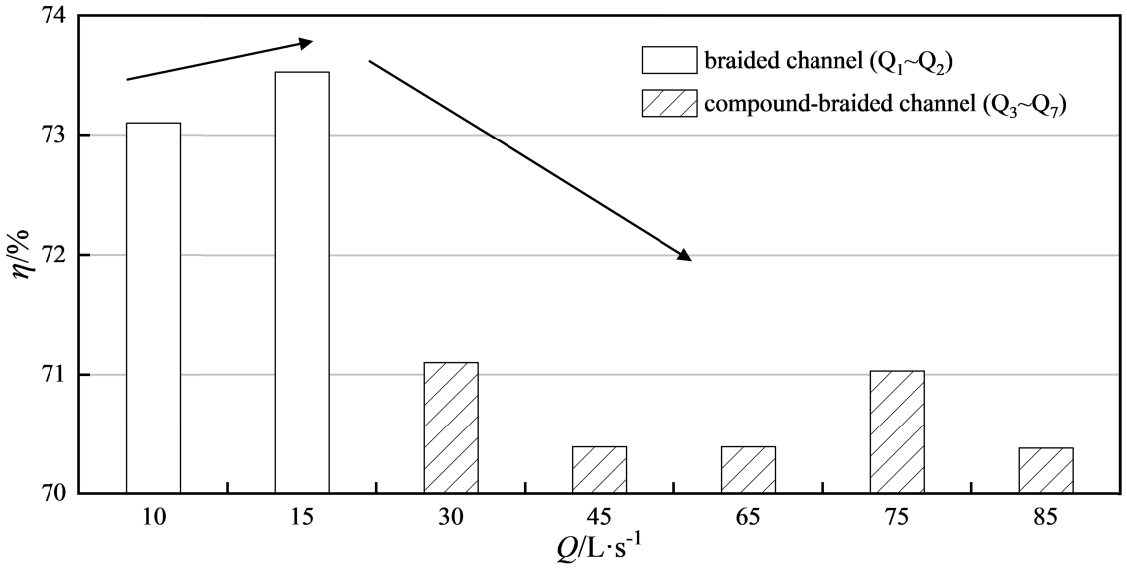

Figure 9. The flow ratio of main branch under different discharges. The filling inside the rectangle represents the different states of the channel, The direction of the arrow represents the increase or decrease in the flow ratio.

The prototype observation and laboratory experiment of the braided river channel both indicate that the diversion ratio η of the main branch gradually increases with increasing discharge, and after discharge reaching the critical value, η remains constant(Du et al., 2016; WANG et al., 2019). According to Figure 9, the flow does not submerged the floodplain under

the condition of small discharge, and the main branch flow of Q_1~Q_2 accounts for over 73%. Moreover, the increase of discharge makes η increase to a certain extent, which is consistent with the previous research results. After the water level rises to form a compound braided channel under the large discharge, η of Q_3~Q_7 is between 70% and 71%, and the diversion ratio of the main branch not only fails to increase but also decreases significantly. The result obtained is inconsistent with the evolution law of the braided channel, but it is consistent with the previous inference about the influence of the changes of the inlet resistance of the main branch on the diversion ratio. This shows that the formation of the compound section by submerging of the floodplain will indeed change the diversion law of the braided channel, which makes the river process of the compound-braided river channel show distinct characteristics from the previous braided channel.

From Figure 9, there is no obvious correlation between the change of the η and the discharge after overbank condition. The boundary resistance of the main channel is sensitive to the change of discharge, but the velocity gradient in the interaction area between the floodplain and the main channel is increased due to the asynchronous changes in resistance between the floodplain and the main channel. This forms a stronger lateral momentum exchange, which maintains the flow capacity of the main branch to a certain extent. The decrease of the main branch diversion ratio caused by overbank is limited, about 3~4%.

4 Conclusion

In this paper, according to the investigation and statistics data from the braided river of Heilongjiang, the generalized flume model is designed. The flow field characteristics, resistance characteristics and branch diversion ratio of the compound bifurcated channel are studied through the flume experiments, and the following conclusions are obtained:

(1) In the bifurcation segment of the compound-braided river channel, the water surface flow pattern and the transverse distribution characteristics of water level can be observed at the same time, which are caused by the influence of central bar diversion and interaction between the floodplain and the main channel. The velocity difference between the floodplain and the main channel aggravates the transverse water surface gradient in the diversion segment, which accelerates the transverse flow of the section and may increase the transverse sediment transport intensity. The vertical vortex caused by center bar diversion through the interaction zone between the floodplain and the main channel should be the main factor, which causes the cross-section sinking flow.

(2) The cross-section vector distribution of flow velocity in the diversion segment is mainly controlled by the diversion effect of the center bar, which completely suppresses the generation of secondary flow. However, the longitudinal cross-section distribution of flow velocity still retains the distribution characteristics of the compound section. Under the combined action of extrusion force and centrifugal force, the longitudinal velocity of the inner floodplain is high, and the transverse flow of the section is violent. If there is no anti-scouring protection of vegetation roots, the center bar may be scoured first, and silted up in the main channel or even the outer floodplain of the downstream. The compound section of the branch is still affected by a certain degree of diversion, and the asymmetric distribution of the secondary flow is caused.

(3) The calculation results of boundary shear stress distribution, based on the interaction of floodplain and main channel, indicate that the resistance of the outer floodplain in both

branches is equivalent. However, from the perspective of the main channel and the inner floodplain, the resistance change of the main branch caused by the increase of flow rate is faster than that of the other branch. In general, after the floodplain is submerged, the section resistance growth of the main branch is significantly greater than that of the other branch. This leads to the diversion ratio of the branch not increasing but decreasing, and the range is very limited. And the diversion ratio no longer decreases with the flow rate continue to increase, basically maintaining a constant value. After the water level rises in the flood season to submerge floodplain, the flow capacity of the branch has a certain improvement, and the braided channel of the compound section may be more conducive to maintaining a relatively stable branch pattern.

5 Discussion

The compound-braided model used in the test is generalized according to the statistics of the braided channel in Heilongjiang. These research conclusions are applicable to the judgment of water level, flow velocity, resistance distribution, and diversion ratio of the straight and asymmetric compound-braided river. For curved braided river, if the reach where the center bar is located is curved, the diversion ratio after the water level overflows also needs to consider the changes of the curved circulation and the mainstream axis. When the tributary is located on the concave bank of the bend, due to the large discharge, the circulation intensity of the bend generated by the curved river section increases, the mainstream axis becomes straight, and the diversion ratio of the branch increases. At the same time, due to the overbank condition, the increase of the flow capacity of the branch is more than that of the main branch, the compound section will further improve the diversion ratio of the branch in the flood season. This causes more intense erosion, which may aggravate the evolution trend of the alternation of the main branch.

Limited by the scope of application of the flow velocity measurement equipment, there are only two groups of bifurcation tests carried out under the condition of non-floodplain. However, even if the flow rate increase is only 5L•s-1, the main branch diversion ratio still has an increase. This is consistent with the existing research and observation conclusions of the diversion ratio of the braided channel, and can be used as a control test group for the diversion ratio data after the floodplain. However, this conclusion is still qualitative, and it is impossible to quantitatively evaluate or calculate the impact of flow or floodplain on the decrease of diversion ratio. Data under more test conditions are needed for further exploration.

During the dry season, both the center bar of the braided river and the floodplain of the compound river remain unsubmerged and usually grows a certain coverage vegetation. The subterranean root system of vegetation roots provides soil consolidation effects, thereby enhancing bank slope erosion resistance. Moreover, the rhizomes and leaves on the ground can significantly increase the water flow resistance. The spatial distribution uniformity of vegetation along both sides of the floodplain and the center bar will also affect the flow velocity distribution in the bifurcation section. In this paper, the experimental conditions of vegetation are not considered, and the calculation of resistance coefficient is deviated from the actual situation. When the research results of this paper are applied or verified in natural river, the factors of vegetation should be considered, such as species, growth, coverage, and distribution uniformity, in view of its great impact on overflow capacity of channel.

Acknowledgments

The authors gratefully acknowledge the support of the Natural Fund Project of Sichuan Science and Technology Department (23NSFSC5355), the Sichuan Univ, State Key Lab Hydraul & Mt River Engn (SKHL2217) and the Open Research Subject of Key Laboratory of Fluid Machinery and Engineering (Xihua University), Sichuan Province (grant number LTJX-2022002).

References

Abbaspour, A. (2020). Experimental investigation on bed shear stress distribution in the roughened compound channel. *Applied Water Science*, *10*(3).

Devi, K., Khatua, K. K., & Khuntia, J. R. (2017). Boundary Shear Stress Distribution for a Two-Stage Asymmetric Compound Channel. *Arabian Journal for Science and Engineering*, *42*(3), 1077–1091. https://doi.org/10.1007/s13369-016-2321-1

Du, Q., Tang, H., Yuan, S., & Xiao, Y. (2016). Predicting flow rate and sediment in bifurcated river branches. *Proceedings of the Institution of Civil Engineers - Water Management*, *169*(4), 156–167. https://doi.org/10.1680/wama.14.00161

HU, C., & JI, Z. (1999). Distribution of Boundary Shear Stress in Compound Cross-section. *Journal of Sediment Research*, *06*, 52–55. https://doi.org/10.16239/j.cnki.0468-155x.1999.06.013

Hua, Z., Gu, L., & Chu, K. (2009). Experiments of Three-Dimensional Flow Structure in Braided Rivers. *Journal of Hydrodynamics*, *21*(2), 228–237. https://doi.org/10.1016/S1001-6058(08)60140-7

KANG, L. (2023). *Flume experimental study on flow capacity of compound bifurcated channel* [Master's thesis]. Xihua University.

Khan, Md. A., & Sharma, N. (2019). Turbulence Study Around Bar in a Braided River Model. *Water Resources*, *46*(3), 353–366. https://doi.org/10.1134/S0097807819030023

LIU, C., YANG, K., & LIU, X. (2012). Two-dimensional analytical solutions to depth-averaged velocity in compound channels with overbank flows. *Journal of Hydraulic Engineering*, *43*(S2), 27–34. https://doi.org/10.13243/j.cnki.slxb.2012.s2.024

Liu, X., Li, L., Hua, Z., Tu, Q., Yang, T., & Zhang, Y. (2019). Flow Dynamics and Contaminant Transport in Y-Shaped River Channel Confluences. *International Journal of Environmental Research and Public Health*, *16*(4), 572. https://doi.org/10.3390/ijerph16040572

Liu, Y. (2003). Development of Research on Essential Characteristics of Meandering Rivers. *Pearl River*, *2*, 1–4.

Luo, F., Liang, Z., & Zhang, D. (1995). Experimental Studies om Division of Flow. *Advances in Water Science*, *01*, 71–75.

Luo, H. (1989). Characteristics of fluvial processes and stability of the braided channel in the middle and lower reaches of the Yangze River. *Journal of Hydraulic Engineering*, *6*, 10–19.

Naik, B., Padhi, E., & Khatua, K. K. (2018). Flow Prediction of Boundary Shear Stress and Depth Average Velocity of a Compound Channel with Narrowing Floodplain. *Iranian Journal of Science and Technology, Transactions of Civil Engineering*, *42*(4), 415–425. https://doi.org/10.1007/s40996-018-0105-4

Proust, S., & Nikora, V. (2018). Flow structure in compound open-channel flows in the presence of transverse currents. *E3S Web of Conferences*, *40*. https://doi.org/10.1051/e3sconf/20184005024

Proust, S., & Nikora, V. I. (2020). Compound open-channel flows: Effects of transverse currents on the flow structure. *Journal of Fluid Mechanics*, *885*. https://doi.org/10.1017/jfm.2019.973

548 Ramamurthy, A. S., & Satish, M. G. (1988). Division of Flow in Short Open Channel Branches.
549 *Journal of Hydraulic Engineering*, *114*(4), 428–438. https://doi.org/10.1061/(ASCE)0733-
550 9429(1988)114:4(428)
551 Spooner, Jake. (2001). *Flow structures in a compound meandering channel with flat and*
552 *natural bedforms* [Ph.D. thesis]. Loughborough University.
553 Stephenson, D., & Kolovopoulos, P. (1990). Effects of Momentum Transfer in Compound
554 Channels. *Journal of Hydraulic Engineering*, *116*(12), 1512–1522.
555 https://doi.org/10.1061/(ASCE)0733-9429(1990)116:12(1512)
556 Tang, H., Zhang, H., & Yuan, S. (2018). Hydrodynamics and contaminant transport on a
557 degraded bed at a 90-degree channel confluence. *Environmental Fluid Mechanics*, *18*(2), 443–
558 463. https://doi.org/10.1007/s10652-017-9562-8
559 Tang, X. (2019). A new apparent shear stress-based approach for predicting discharge in
560 uniformly roughened straight compound channels. *Flow Measurement and Instrumentation*, *65*,
561 280–287. https://doi.org/10.1016/j.flowmeasinst.2019.01.012
562 TONG, C., YAN, Y., MENG, Y., & YUE, L. (2011). Methods of evaluating flow diversion ratio
563 of bifurcated rivers. *Advances in Science and Technoligy of Water Resource*, *31*(06), 7-9+90.
564 WANG, Z., LI, Y., DONG, Z., ZHUANG, W., WENG, S., & ZHANG, J. (2019). Influencing
565 factors of flow diversion ratio in plain river networks of Taihu Lake Basin. *Water Resources*
566 *Protection*, *35*(4), 49-54+75.
567 Yonesi, H. A., Parsaie, A., Arshia, A., & Shamsi, Z. (2022). Discharge modeling in compound
568 channels with non-prismatic floodplains using GMDH and MARS models. *Water Supply*, *22*(4),
569 4400–4421. https://doi.org/10.2166/ws.2022.058

ZHANG, J., WANG, P., HU, J., & WANG, M. (2021). Experimental Study on the Characteristics of Near-Bottom Flow in Bifurcated Channel. *Science Technology and Engineering*, *21*(8), 3297–3303.

ZHAO, C., WANG, pingyi, WANG, M., & CHEN, Y. (2022). Experimental study on flow law of branching channel under different branching ratios. *Port & Waterway Engineering*, *05*, 84–90. https://doi.org/10.16233/j.cnki.issn1002-4972.20220418.026

Г.В.Zheleznyakov. (1956). *On the Bases of Hydraulics for Method of Hydrometry of River*. China Water Conservacy Press.